Controlling the contributions to high-order harmonic generation from different nuclei of N_2 with an orthogonally polarized two-color laser field*

Hui Du(杜慧), Xue-Fei Pan(潘雪飞), Hai-Feng Liu(刘海凤), Hong-Dan Zhang(张宏丹), Jun Zhang(张军), Jing Guo(郭静), and Xue-Shen Liu(刘学深)†

Institute of Atomic and Molecular Physics, Jilin University, Changchun 130012, *China*

(Received 7 April 2016; revised manuscript received 25 April 2016; published online 20 July 2016)

The generation of high-order harmonic and the attosecond pulse of the N_2 molecule with an orthogonally polarized two-color laser field are investigated by the strong-field Lewenstein model. We show that the control of contributions to high-order harmonic generation (HHG) from different nuclei is realized by properly selecting the relative phase. When the relative phase is chosen to be $\varphi = 0.4\pi$, the contribution to HHG from one nucleus is much more than that from another. Interference between two nuclei can be suppressed greatly; a supercontinuum spectrum of HHG appears from 40 eV to 125 eV. The underlying physical mechanism is well explained by the time–frequency analysis and the semi-classical three-step model with a finite initial transverse velocity. By superposing several orders of harmonics, an isolated attosecond pulse with a duration of 80 as can be generated.

Keywords: high-order harmonic generation, orthogonally polarized two-color laser field, attosecond pulse

PACS: 32.80.Rm, 42.65.Ky, 42.65.Re **DOI:** 10.1088/1674-1056/25/9/093202

1. Introduction

With the fast development of femtosecond laser technology, recent years have witnessed great success both in research and application of high-order harmonic generation (HHG).[1–4] High-order harmonic radiation has been a powerful tool to generate attosecond pulses[5–8] and coherent soft x-ray source,[9] to probe ultrafast electronic dynamics,[10,11] and to reveal structures of molecular orbitals.[12,13] The basic understanding of the formation for attosecond pulse train in HHG has been provided by a semi-classical three-step model.[14–16] An electron in an atom is ionized by tunneling through the effective potential barrier, then it oscillates freely under the drive of the electronic field, and after sign reversal of the field, it may recollide with its parent ion, emitting a harmonic photon simultaneously whose energy corresponds to the sum of ionization energy and the kinetic energy of the electron.

In recent decades, a lot of advanced techniques have been proposed to generate an isolated attosecond pulse both in experiment and theory, such as few-cycle laser pulses,[17,18] two-color field,[19,20] and polarization gating.[21–23] As a kind of polarization gating scheme, the orthogonally polarized two-color (OPTC) laser fields by superimposing a driving field and its orthogonally polarized second harmonic have been proposed as a simple yet effective approach to steer the electronic dynamics.[24–27] Kim *et al.*[28,29] proposed an efficient method to control the quantum path by appropriately changing the relative phase of the OPTC laser field, leading to a continuous HHG spectrum and a regular attosecond pulse. It has been demonstrated that correlated electron dynamics are sensitively dependent on the relative phase of the OPTC laser field in non-sequential double ionization (NSDI) and realized the control of electrons recollision as well as emission in space and time with sub-laser-cycle and attosecond precision.[30,31] Xie[32] proposed a two-dimensional interferometry based on the electron wave-packet interference by using a cycle-shaped OPTC laser field, in which different types of interferences can be easily disentangled into different directions in the measured 2D photoelectron momentum spectrum. A powerful scheme with phase-controlled OPTC laser fields has also been proposed experimentally to control the interference between electron wave packets released at different times.[33] Moreover, the effect of electron diffraction[34] and the image of atomic and molecular orbital features by the measurements of HHG spectra[35,36] were also reported with such pulses.

In this paper, we theoretically investigate the HHG of the N_2 molecule in an OPTC laser field by the strong-field Lewenstein model. We find that the control of contributions to harmonic radiation from different nuclei is realized by properly selecting the relative phase. The interference between two nuclei can be suppressed greatly by enhancing contribution from one nucleus and inhibiting contribution from another nucleus, which is very beneficial to generate a clean and regular harmonic spectrum. As a result, an isolated attosecond pulse with a bandwidth of 80 as can be generated directly by the superposition of the supercontinuum harmonics.

*Project supported by the National Natural Science Foundation of China (Grant Nos. 11271158, 61575077, and 11574117).

†Corresponding author. E-mail: liuxs@jlu.edu.cn

© 2016 Chinese Physical Society and IOP Publishing Ltd

2. Model

We demonstrate the generation of high-order harmonic and the attosecond pulse of N_2 molecules by the strong-field Lewenstein model.[14,21,37] The transition amplitude for HHG can be calculated by the integral

$$\begin{aligned} r(t) &= \mathrm{i}\int_0^{\infty} \mathrm{d}\tau \left(\frac{\pi}{\varepsilon+\mathrm{i}\frac{\tau}{2}}\right)^{3/2} \times d^*_{\mathrm{rec}}[p_{\mathrm{st}}(t,\tau)-A(t)] \\ &\times d_{\mathrm{ion}}[p_{\mathrm{st}}(t,\tau)-A(t-\tau)]E(t-\tau) \\ &\times \exp[-\mathrm{i}S(p_{\mathrm{st}},t,\tau)]+\mathrm{c.c.}. \end{aligned} \tag{1}$$

The transition amplitude contains the information of HHG which is in good agreement with the semi-classical three-step model: $d_{\mathrm{ion}}[p_{\mathrm{st}}(t,\tau)-A(t-\tau)]E(t-\tau)$, depicts the progress of electrons emitted from ground state to the continuous state; $\exp[-\mathrm{i}S(p_{\mathrm{st}},t,\tau)]$ represents the motion of the freed electrons without the interaction of Coulomb potential; $d_{\mathrm{rec}}[p_{\mathrm{st}}(t,\tau)-A(t)]$ is the transition dipole of the freed electrons turning back to the ion parent. ε is a positive regularization constant, τ is the traveling time of free electron between ionization and recombination. $E(t)$ is the electric field of the laser pulse and $A(t)$ is the associated vector potential. $p_{\mathrm{st}}(t,\tau)$ is the stationary momentum obtained by the stationary points integral algorithm. $S(p_{\mathrm{st}},t,\tau)$ is the quasi-classical action of the electron.

It has been demonstrated that the quasi-classical action $S(p_{\mathrm{st}},t,\tau)$ has been considered in the molecular structure information,[38] which incorporates four possible recombination scenarios as shown in Fig. 1, where C_1 and C_2 are the nuclei of N_2 molecule and R is the inter-nuclear distance. Figure 1 shows that the electron leaves and returns to the same nucleus, or the electron is emitted from a nucleus and recombines with another nucleus.[38] Since the HHG mainly depends on the progress of recombination, one may distinguish two main scenarios: the progress of an ionized electron that recombines with the nucleus C_1 and the progress of an ionized electron that recombines with the nucleus C_2. On this basis, we investigate the contributions to HHG from two nuclei of N_2 molecule, respectively, to illustrate the characteristics of the harmonic spectrums.

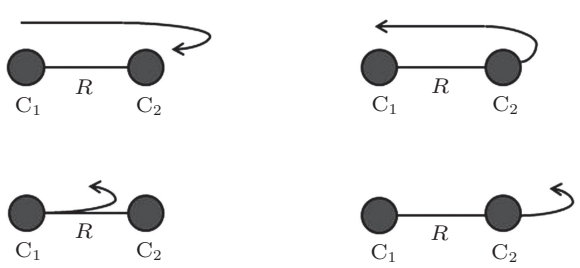


Fig. 1. Four possible recombination scenarios of the ionized electron that returns to the parent ion. C_1 and C_2 are the nuclei of N_2 molecule.

We investigate the HHG of N_2 molecule by an OPTC laser field, in which the highest occupied molecular orbital (HOMO) constructed by the GAMESS-UK package[39,40] is taken into account. The transition amplitude can be calculated along the x and y directions

$$\begin{aligned} x(t) &= \mathrm{i}\int_0^{\infty} \mathrm{d}\tau \left(\frac{\pi}{\varepsilon+\mathrm{i}\frac{\tau}{2}}\right)^{3/2} \times d^*_{\mathrm{rec}x}[p_{\mathrm{st}}(t,\tau)-A(t)] \\ &\times \{d_{\mathrm{ion}x}[p_{\mathrm{st}}(t,\tau)-A(t-\tau)]E_x(t-\tau) \\ &+ d_{\mathrm{ion}y}[p_{\mathrm{st}}(t,\tau)-A(t-\tau)]E_y(t-\tau)\} \\ &\times \exp[-\mathrm{i}S(p_{\mathrm{st}},t,\tau)]+\mathrm{c.c.}, \end{aligned} \tag{2}$$

$$\begin{aligned} y(t) &= \mathrm{i}\int_0^{\infty} \mathrm{d}\tau \left(\frac{\pi}{\varepsilon+\mathrm{i}\frac{\tau}{2}}\right)^{3/2} \times d^*_{\mathrm{rec}y}[p_{\mathrm{st}}(t,\tau)-A(t)] \\ &\times \{d_{\mathrm{ion}x}[p_{\mathrm{st}}(t,\tau)-A(t-\tau)]E_x(t-\tau) \\ &+ d_{\mathrm{ion}y}[p_{\mathrm{st}}(t,\tau)-A(t-\tau)]E_y(t-\tau)\} \\ &\times \exp[-\mathrm{i}S(p_{\mathrm{st}},t,\tau)]+\mathrm{c.c.}, \end{aligned} \tag{3}$$

where $E_x(t)$ and $E_y(t)$ are the x and y components of the OPTC laser field, and $p_{\mathrm{st}}(t,\tau)$ is the stationary momentum obtained by the stationary points integral algorithm. The quasi-classical action $S(p_{\mathrm{st}},t,\tau)$ at the stationary points can be calculated by

$$\begin{aligned} S(p_{\mathrm{st}},t,\tau) &= \tau I_p - \frac{1}{2}[p^2_{\mathrm{st,x}}(t,\tau)+p^2_{\mathrm{st,y}}(t,\tau)] \\ &+ \frac{1}{2}\int_{t-\tau}^{t}[A_x^2(t'')+A_y^2(t'')]\,\mathrm{d}t''. \end{aligned} \tag{4}$$

The harmonic spectrum intensity is obtained by Fourier transforming the time-dependent dipole acceleration

$$P_a(\omega) = \left|\frac{1}{T-t_0}\int_{t_0}^{T}[x(t)\boldsymbol{e}_x+y(t)\boldsymbol{e}_y]\,\mathrm{e}^{-\mathrm{i}\omega t}\,\mathrm{d}t\right|^2. \tag{5}$$

The temporal profile of an attosecond pulse can be obtained by superposing several harmonics in x and y directions as follows:

$$I_x(t) = |\Sigma a_{qx}\,\mathrm{e}^{\mathrm{i}\omega q t}|^2, \tag{6}$$

$$I_y(t) = |\Sigma a_{qy}\,\mathrm{e}^{\mathrm{i}\omega q t}|^2, \tag{7}$$

where $a_{qx} = \int x(t)\,\mathrm{e}^{-\mathrm{i}q\omega t}\,\mathrm{d}t$ and $a_{qy} = \int y(t)\,\mathrm{e}^{-\mathrm{i}q\omega t}\,\mathrm{d}t$, and q is the harmonic order.

It is known that electrons ionized without an initial transverse velocity will miss the parent ion in the elliptical polarization laser field and a semi-classical three-step model with a proper initial transverse velocity is introduced in our paper to explain the underlying mechanism of the progress of HHG, in which the transverse displacement caused by the external field is compensated by an initial transverse velocity.[41,42]

3. Numerical results

We demonstrate the contributions to the high-harmonic yield from different nuclei of N_2 molecule in an OPTC laser field, which is composed of a 400-nm linearly polarized field along the x axis and a 800-nm linearly polarized field along the y axis. The synthesized field can be expressed as

$$E(t) = \boldsymbol{x}E_0 \exp\left[-2\ln(2)\left(\frac{t}{\tau}\right)^2\right]\cos(\omega_1 t)$$

$$+\boldsymbol{y}E_0 \exp\left[-2\ln(2)\left(\frac{t}{\tau}\right)^2\right]\cos(\omega_2 t+\varphi). \quad (8)$$

The peak intensities E_0 of the two pulses are equal, which is chosen as 7×10^{14} W/cm^2. The carrier frequency $\omega_1 = 0.1138$ a.u. (400 nm in wavelength) and $\omega_2 = 0.0569$ a.u. (800 nm in wavelength). $\tau = 3$ fs is the full width at half maximum (FWHM) of the laser field. $\boldsymbol{x}$ and $\boldsymbol{y}$ are the polarization vectors. φ is the relative phase between the two components.

Figure 2(a) shows the electric field of the OPTC laser field (black solid line) with $\varphi = 0$. The green dashed line is the linearly polarized 400-nm field along the x axis and the blue dotted line is the linearly polarized 800-nm field along the y axis. The ionized electron is driven by the electronic force in both x and y directions so that the motion along the x axis is mainly affected by the linearly polarized 400-nm field and the motion along the y axis is mainly affected by the linearly polarized 800-nm field, respectively. Figure 2(b) shows the high-order harmonic spectrum obtained by summing up the intensities of the x and y components in the OPTC laser field with a relative phase $\varphi = 0$. It shows that there is an irregular spectrum with a cut-off energy of about 165 eV. Moreover, the intensity of the spectrum between 107–122 eV shows an obvious subsidence and an interference minimum appears around 116 eV.

To explain the underlying mechanism of the HHG, we illustrate the emission time of the harmonics in terms of the time–frequency analysis of the dipole acceleration along the x and y directions, which is shown in Figs. 3(a) and 3(b), respectively. It is shown that the emission peaks in both directions are similar and the intensity of the emission peaks in the y direction is a little stronger than that in the x direction, thus we only demonstrate the HHG progress along the y direction for convenience if not explicitly stated. Figure 3(b) shows that there are three emission peaks marked as A, B, and C. There are two quantum paths for each emission peak: the quantum path with earlier ionization time but later emission time is the long path, and the other path with later ionization time but earlier emission time is the short path. The maximum kinetic energy of the emission peak B located around 0.2 O.C. reaches 165 eV, which corresponds to the cut-off energy of the spectrum shown in Fig. 2(a). Due to the higher intensities, emission peaks B and C make a major contribution to HHG, of which the short paths are suppressed and the long paths are selected. Figure 3(c) shows the dependence of the energy on the ionization and emission times by the semiclassical three-step model with a finite initial transverse velocity. This indicates that the electrons are mainly ionized around -1 O.C., -0.4 O.C., 0.1 O.C., and the electron recombination takes place around peak A′, B′, and C′, which corresponds to the emission peaks A, B, and C shown in Fig. 3(b). The electrons are ionized at around -0.4 O.C. and return at around 0.2 O.C. with the maximum energy of 165 eV. Figure 3(d) shows the electron trajectories with finite initial transverse velocities, which depicts that the freed electrons are driven by the electronic field and finally move back to the origin.

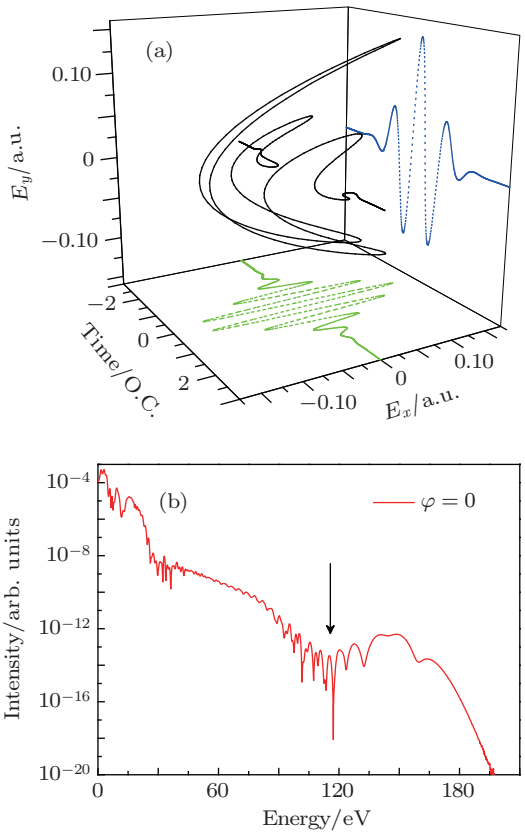


Fig. 2. (color online) (a) Electric field of the orthogonally polarized two-color laser field with a relative phase $\varphi = 0$; (b) harmonic spectrum obtained by summing up the intensities of the x and y components in the OPTC laser field with a relative phase $\varphi = 0$.

Figure 4 shows the Lissajous diagrams of OPTC laser field with different relative phases varying from 0 to π by an interval of $\pi/8$, which indicates the trajectories of the electronic field vectors in one optical cycle. In the case of $\varphi = 0$, figure 4(a) shows that the trajectory of the electronic field vector shows a periodic oscillation and the electronic field of two components reaches the peaks simultaneously, resulting in the matched motions along x and y directions. One can see that the two components cannot pass through zero at the same time. In other words, when an ionized electron is driven across zero point along the x direction, the motion along the y direction cannot return to the nucleus region; therefore the ionized electron has to experience much more time for recollision, which corresponds to the long path of the trajectory. Thus, in the case of $\varphi = 0$, the long path is selected and short path is suppressed as discussed in Fig. 3(b).

When the relative phase changes from 0 to 0.825π, Lissajous diagrams of OPTC laser field are shown in Figs. 3(b)–3(h), which resemble a bow tie and become elongated or contracted trajectories. Especially in the case of $\varphi = 0.5\pi$, figure 4(e) shows that the two crossed linear regions appear

around the origin, alternately reversing its direction every half an optical cycle. Although the motion along the x and y directions is not matched, the ionized electron can be driven back to the nucleus region along the x and y directions simultaneously. Just like the circumstance of the short path in one-color linearly polarized laser field, the electron emitted in the linear region can be captured directly by the nucleus after sign reversal of the field, which corresponds to the short path of the trajectory. Thus, in the case of $\varphi = 0.5\pi$, the short path is selected and long path is suppressed.

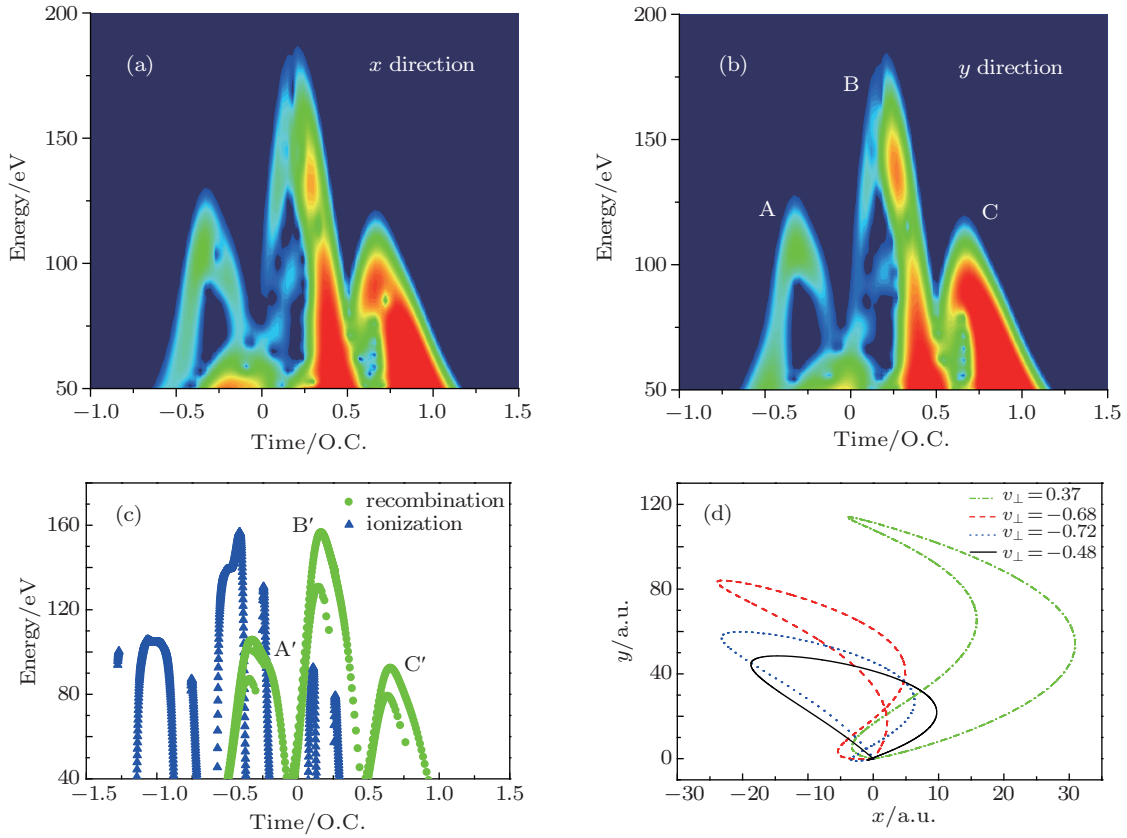


Fig. 3. (color online) Time–frequency distribution of the harmonics along (a) the x and (b) y directions; (c) dependence of energy on the ionization (solid blue triangles) and emission times (solid green circles) in the OPTC laser field with a relative phase $\varphi = 0$; (d) the corresponding electron trajectories with finite initial transverse velocities.

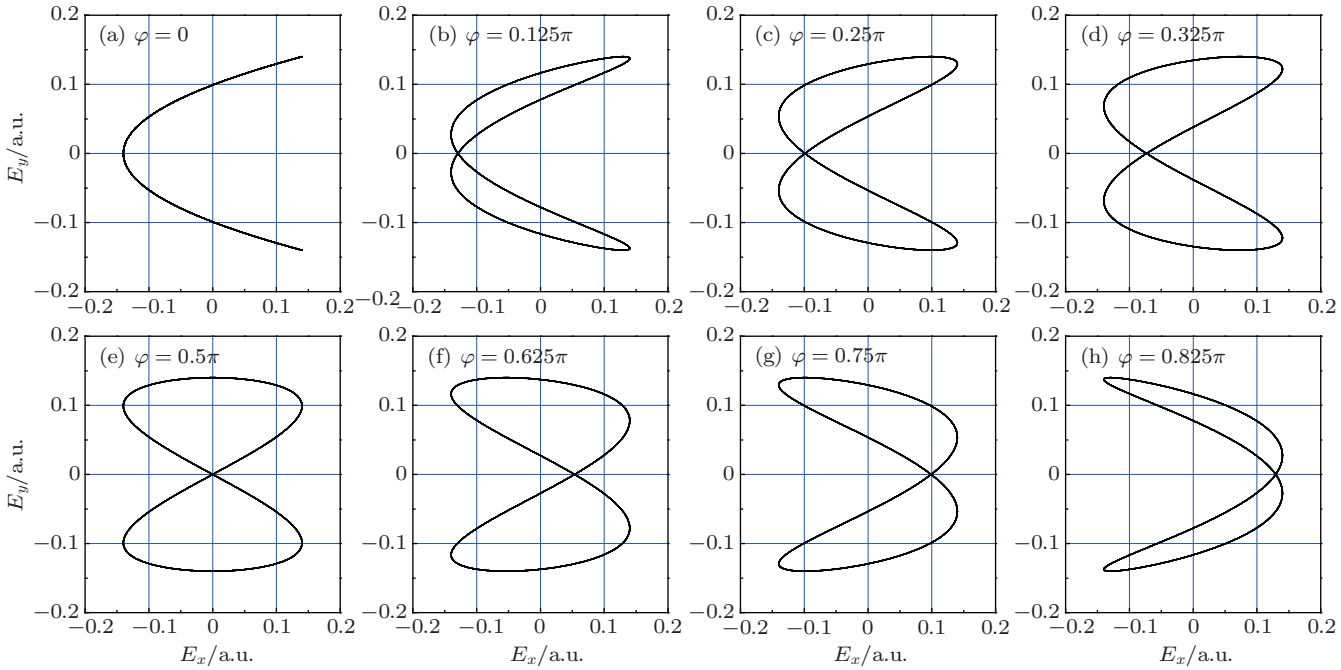


Fig. 4. (color online) Lissajous diagrams of OPTC laser field with different relative phases φ varying from 0 to π by an interval of $\pi/8$. (a) $\varphi = 0$, (b) $\varphi = 0.125\pi$, (c) $\varphi = 0.25\pi$, (d) $\varphi = 0.325\pi$, (e) $\varphi = 0.5\pi$, (f) $\varphi = 0.625\pi$, (g) $\varphi = 0.75\pi$, (h) $\varphi = 0.825\pi$.

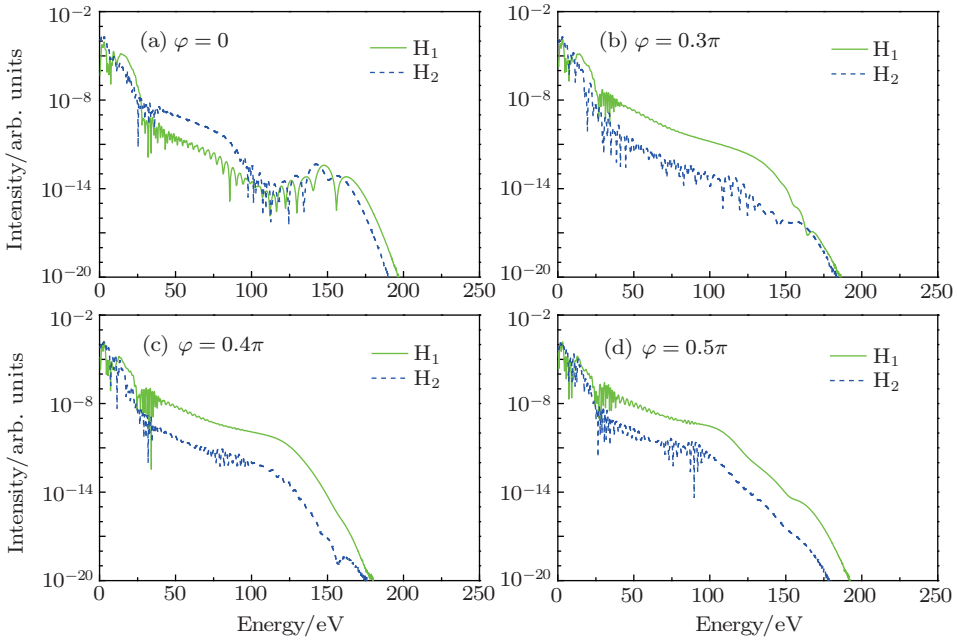


Fig. 5. (color online) High-order harmonic generation when the electron recombines with different nuclei of N_2 molecule along the y direction in the OPTC laser field with different relative phases (a) $\varphi = 0$, (b) $\varphi = 0.3\pi$, (c) $\varphi = 0.4\pi$, (d) $\varphi = 0.5\pi$. The green solid line H_1 shows the HHG when the electron recombines with the nucleus C_1 and the blue dashed line H_2 shows the HHG when the electron recombines with the nucleus C_2, respectively.

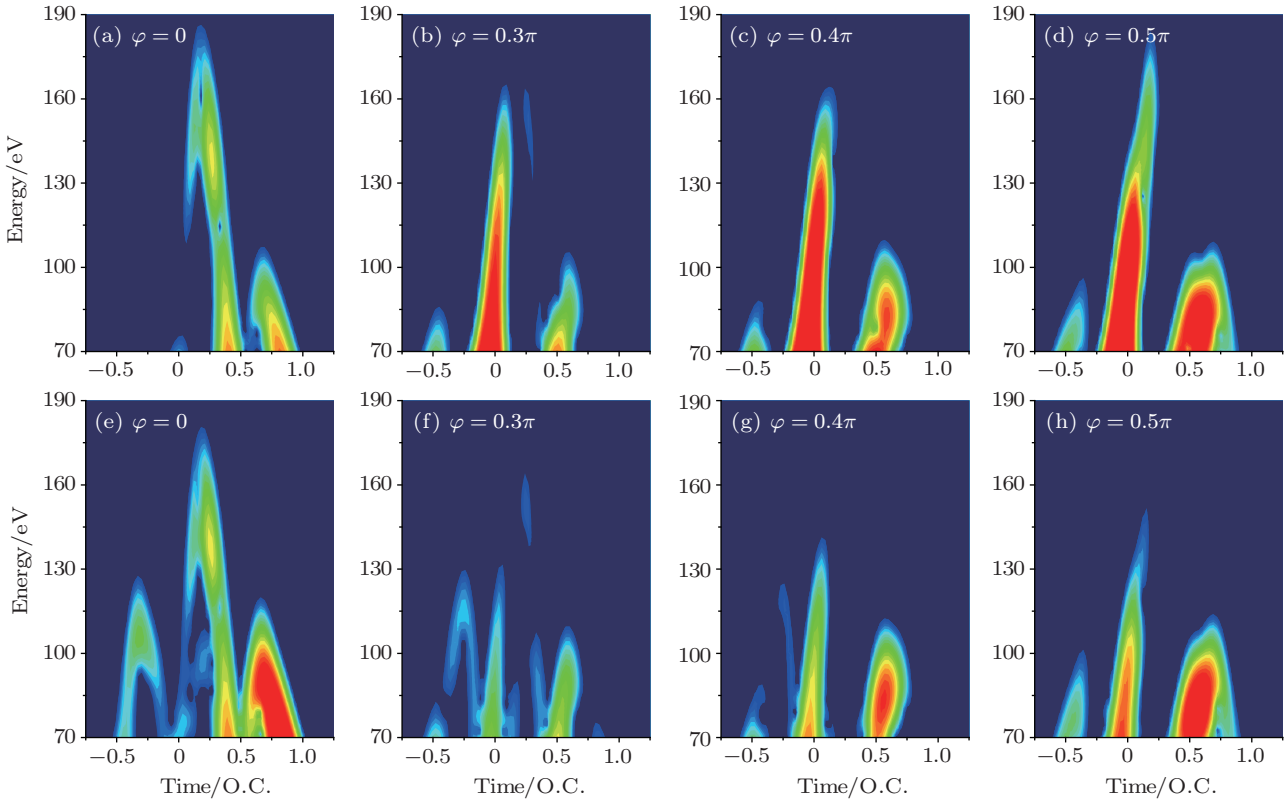


Fig. 6. (color online) Time–frequency distributions of the high-harmonic spectrum along the y direction when the electron recombines with the nucleus C_1 (a)–(d) and the nucleus C_2 (e)–(h) of N_2 molecule in the OPTC laser field with different relative phases $\varphi = 0$, $\varphi = 0.3\pi$, $\varphi = 0.4\pi$, and $\varphi = 0.5\pi$, respectively.

Figure 5 shows the HHG along the y direction when the electron recombines with the nuclei C_1 and C_2 in OPTC laser field with different relative phases, which can distinguish the contributions to HHG from different nuclei of the N_2. The green solid line H_1 shows the HHG when the electron recombines with the nucleus C_1 and the blue dashed line H_2 shows the HHG when the electron recombines with the nucleus C_2, respectively. For $\varphi = 0$, figure 5(a) shows that the contribution to HHG from the nucleus C_1 is a little smaller than that from the nucleus C_2. With increasing value of relative phase, fig-

ures 5(b)–5(d) show that the intensity of spectrum generated by electrons recombined with the nucleus C_1 is gradually enhanced while the contribution to HHG from C_2 is suppressed. This may provide very good enlightenment that the interference between two nuclei can be suppressed by enhancing contribution of one nucleus and inhibiting the contribution of another nucleus, which is very beneficial to generate a clean and regular harmonic spectrum.

We demonstrate the time–frequency distributions of the high-harmonic spectrum along the y direction when the electron recombines with the nucleus C_1 in Figs. 6(a)–6(d) and the nucleus C_2 in Figs. 6(e)–6(h) of N_2 molecule in OPTC laser field with different relative phases of $\varphi = 0$, $\varphi = 0.3\pi$, $\varphi = 0.4\pi$, and $\varphi = 0.5\pi$, respectively. For the case of $\varphi = 0$, figures 6(a) and 6(e) show that the intensity of emission peaks contributed by the electron recombined with the nucleus C_1 is a little smaller than that with the nucleus C_2. For the case of $\varphi = 0.3\pi$, figures 6(b) and 6(f) show that the intensity of emission peaks contributed by the electron recombined with the nucleus C_2 is suppressed and the emission peaks contributed by the electron recombined with the nucleus C_1 dominate the major contribution. For cases of $\varphi = 0.4\pi$ and $\varphi = 0.5\pi$, a similar phenomenon can be observed. From Fig. 6 we can see that, with the increase in the phases, the short path is selected and the long path is suppressed, which is in good agreement with the discussion of Fig. 4.

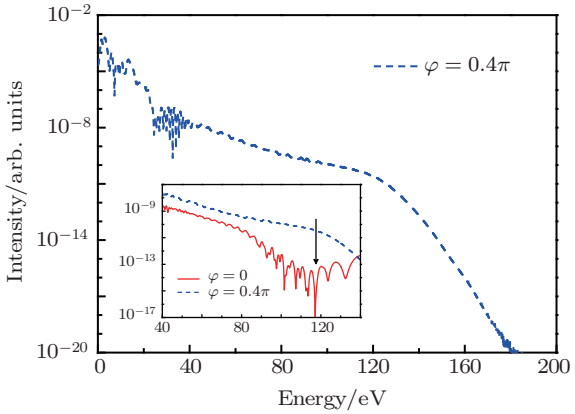


Fig. 7. (color online) Harmonic spectrum obtained by summing up the intensities of the x and y components in the OPTC laser field with $\varphi = 0.4\pi$. The inset shows the comparison of the spectrums between 40–140 eV generated by the OPTC laser field with $\varphi = 0$ (red solid line) and $\varphi = 0.4\pi$ (blue dashed line).

We know that the interference between two nuclei can be suppressed by enhancing the contribution of one nucleus and inhibiting the contribution of another nucleus. In Fig. 7, we show that a smooth and strong harmonic spectrum is obtained by summing up the intensities of the x and y components with $\varphi = 0.4\pi$. We can see that a continuum spectrum can be achieved from 40 eV to 125 eV. The comparison of the spectrums between 40–140 eV for $\varphi = 0$ and $\varphi = 0.4\pi$ is presented in the inset of Fig. 7, which shows that the intensity of the spectrum for $\varphi = 0.4\pi$ is greatly enhanced compared to that for $\varphi = 0$, and the subsidence of spectrum plateau as well as the interference minimum are absent.

Figure 8 shows the temporal profiles of the attosecond pulses generated by superposing several bandwidths of the harmonics of the spectrums for the relative phases $\varphi = 0$ and $\varphi = 0.4\pi$. For the case of $\varphi = 0$, the temporal profile of the selected shortest attosecond pulse with the duration of 147 as is shown in Fig. 8(a) by superposing the harmonics from 120 eV–160 eV. For the case of $\varphi = 0.4\pi$, the plateau structure is a supercontinuum spectrum with less modulation. Thus, an isolated attosecond pulse can be generated by superposing any range of the harmonic spectrum. By superposing the harmonics in the range of 68 eV–106 eV, an isolated attosecond pulse with the duration of about 80 as is generated as shown in Fig. 8(b).

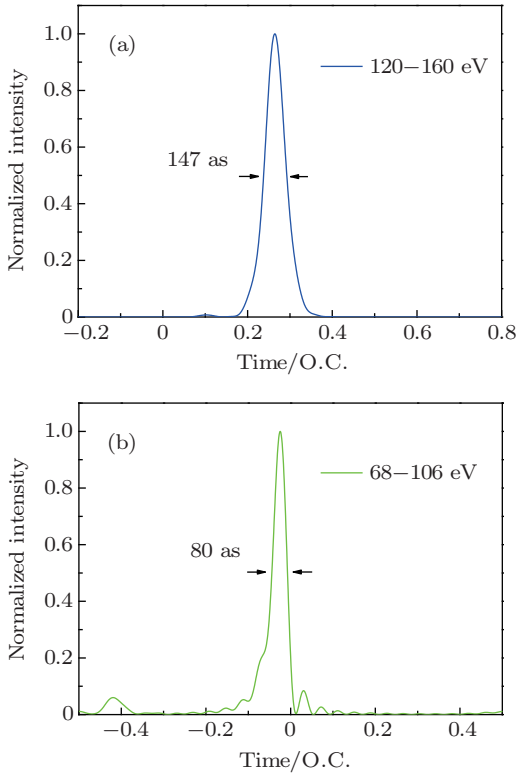


Fig. 8. (color online) Temporal profiles of the attosecond pulses generated by superposing the harmonics for the relative phase (a) $\varphi = 0$ and (b) $\varphi = 0.4\pi$.

4. Conclusions

We theoretically investigate the generation of high-order harmonic and attosecond pulse of the N_2 molecule in an orthogonally polarized two-color laser field by the strong-field Lewenstein model. By properly selecting the relative phase, the control of contributions to HHG from different nuclei of the N_2 is realized and a smooth and strong harmonic spectrum is obtained with $\varphi = 0.4\pi$. A continuum spectrum can be achieved from 40 eV to 125 eV and the subsidence of spectrum plateau as well as the interference minimum is absent.

The time–frequency analysis and the semi-classical three-step model with a finite initial transverse velocity are used to illustrate the physical mechanism of the HHG. By superposing several bandwidths of harmonic spectrum, an isolated 80-as pulse can be generated directly.

References

[1] Le A T, Wei H, Jin C and Lin C D 2016 *J. Phys. B: At. Mol. Opt. Phys.* **49** 053001
[2] Zhong S Y, He X K, Teng H, Ye P, Wang L F, He P and Wei Z Y 2016 *Chin. Phys. B* **25** 023301
[3] Zhang J, Du H, Liu H F, Guo J and Liu X S 2016 *Opt. Commun.* **366** 457
[4] Milošević D B 2015 *Phys. Rev. A* **92** 043827
[5] Wu J, Zhang G T, Xia C L and Liu X S 2010 *Phys. Rev. A* **82** 013411
[6] Ge X L, Du H, Wang Q, Guo J and Liu X S 2015 *Chin. Phys. B* **24** 023201
[7] Cao X, Jiang S, Yu C, Wang Y, Bai L and Lu R 2014 *Opt. Express* **22** 26153
[8] Du H, Wang H and Hu B 2010 *Phys. Rev. A* **81** 063813
[9] Bartels R A, Paul A, Green H, *et al.* 2002 *Science* **297** 376
[10] Maurer J, Dimitrovski D, Christensen L, Madsen L B and Stapelfeldt H 2012 *Phys. Rev. Lett.* **109** 123001
[11] Goulielmakis E, Loh Z H, Wirth A, *et al.* 2010 *Nature* **466** 739
[12] Zhang C P and Miao X Y 2015 *Chin. Phys. B* **24** 043302
[13] Zhang B, Yuan J and Zhao Z 2014 *Phys. Rev. A* **90** 035402
[14] Lewenstein M, Balcou P, Ivanov M Y, L'Huillier A and Corkum P B 1994 *Phys. Rev. A* **49** 2117
[15] Corkum P B 1993 *Phys. Rev. Lett.* **71** 1994
[16] Schafer K J, Yang B, DiMauro L F and Kulander K C 1993 *Phys. Rev. Lett.* **70** 1599
[17] Goulielmakis E, Schultze M, Hofstetter M, *et al.* 2008 *Science* **320** 1614
[18] Christov I P, Murnane M M and Kapteyn H C 1997 *Phys. Rev. Lett.* **78** 1251
[19] Feng L and Chu T 2011 *Phys. Rev. A* **84** 053853
[20] Li P C, Laughlin C and Chu S I 2014 *Phys. Rev. A* **89** 023431
[21] Chang Z 2005 *Phys. Rev. A* **71** 023813
[22] Yuan K J and Bandrauk A D 2015 *Phys. Rev. A* **92** 063401
[23] Jiao Z H, Wang G L, Li P C and Zhou X X 2014 *Phys. Rev. A* **90** 025401
[24] Zheng Y, Diao H, Zeng Z, Ge X, Li R and Xu Z 2015 *Phys. Rev. A* **92** 033417
[25] Brugnera L, Hoffmann D J, Siegel T, Frank F, Zaïr A, Tisch J W G and Marangos J P 2011 *Phys. Rev. Lett.* **107** 153902
[26] Zhang L, Xie X, Roither S, Kartashov D, *et al.* 2014 *Phys. Rev. A* **90** 061401(R)
[27] Yuan Z, Ye D, Xia Q, Liu J and Fu L 2015 *Phys. Rev. A* **91** 063417
[28] Kim C M, Kim I J and Nam C H 2005 *Phys. Rev. A* **72** 033817
[29] Kim C M and Nam C H 2006 *J. Phys. B: At. Mol. Opt. Phys.* **39** 3199
[30] Chen L, Zhou Y, Huang C, Zhang Q and Lu P 2013 *Phys. Rev. A* **88** 043425
[31] Zhang L, Xie X, Roither S, *et al.* 2014 *Phys. Rev. Lett.* **112** 193002
[32] Xie X 2015 *Phys. Rev. Lett.* **114** 173003
[33] Richter M, Kunitski M, Schöffler M, *et al.* 2015 *Phys. Rev. Lett.* **114** 143001
[34] Murray R, Ruiz C, Marangos J P and Ivanov M Y 2010 *J. Phys. B: At. Mol. Opt. Phys.* **43** 135601
[35] Shafir D, Mairesse Y, Villeneuve D M, Corkum P B and Dudovich N 2009 *Nat. Phys.* **5** 412
[36] Niikura H, Dudovich N, Villeneuve D M and Corkum P B 2010 *Phys. Rev. Lett.* **105** 053003
[37] Priori E, Cerullo G, Nisoli M, *et al.* 2000 *Phys. Rev. A* **61** 063801
[38] Figueira de Morisson Faria C 2009 *Laser Phys.* **19** 797
[39] GAMESS-UK is a package of ab initio programs (see http://www.cfs.dl.ac.uk/gamess-uk/index.shtml)
[40] Guest M F, Bush I J, Van Dam H J J, *et al.* 2005 *J. Mol. Phys.* **103** 719
[41] Sansone G 2009 *Phys. Rev. A* **79** 053410
[42] Möller M, Cheng Y, Khan S D, *et al.* 2012 *Phys. Rev. A* **86** 011401(R)